Effect of S_1 Torsional Dynamics on the Time-Resolved Fluorescence Spectra of 9,9′-Bianthryl in Solution

Karsten Elich, Minoru Kitazawa, and Tadashi Okada*

Department of Chemistry, Faculty of Engineering Science, Osaka University, Toyonaka, Osaka 560, Japan

Rüdiger Wortmann

Institut für Physikalische Chemie, Universität Mainz, Jakob Welder-Weg 11, D-55099 Mainz, Germany

Received: November 25, 1996[⊗]

Time-resolved fluorescence spectra of 9,9′-bianthryl (BA) were measured in methylcyclohexane (MCH) and a Decalin−isooctane (D−ISOO) mixture at several temperatures between 127 and 200 K. A suitable choice of the excitation wavelength makes it possible to observe a maximum manifestation of the S_1 torsional dynamics. A quantitative simulation of the time-resolved fluorescence spectra could be achieved based on the description of the torsional relaxation by a Smoluchowski equation. Besides, the band shape analysis enabled the determination of the effective S_1 torsional potential as well as the temperature dependence of the friction coefficient related to the internal torsional motion. The friction coefficient ζ shows a power law dependence on the shear viscosity η, $\zeta \propto \eta^a$, with $a = 0.62$.

Introduction

Large amplitude motions (LAM), which represent a characteristic feature of flexible molecules, are involved in many photophysical processes. Examples are cis−trans-isomerization,[1,2] intramolecular electron[3] and proton transfer,[4] intramolecular vibrational relaxation,[5] and other nonradiative processes.[6] In the liquid phase, the large amplitude motion reflects sensitively the interaction between solute and solvent molecules, providing a good measure of the solvent structure and dynamics. Therefore, the excited-state dynamics of molecules with LAM degrees of freedom has often been investigated to test theoretical models of unimolecular reactions.[7−12] Especially, the dependence of the microscopic friction coefficient on the macroscopic shear viscosity and the importance of non-Markovian effects[13] have attracted considerable interest.

The potentials governing the large amplitude motion could be quantitatively determined for isolated ultracold molecules by analysis of their laser-induced fluorescence (LIF) excitation and dispersed fluorescence spectra obtained in a molecular beam experiment.[2] In many molecular systems, strongly differing LAM potentials were found for the S_0 and the S_1 states.[2,14−19] However, this phenomenon often causes a strong broadening of the optical spectra measured in solution, which renders more difficult the extraction of quantitative information about the vibronic structure as well as the LAM potentials in solution.

In preceding studies,[20,21] we have shown for molecules with one LAM degree of freedom (e.g., torsional angle of biaryl type molecules) that the separation of spectral structures arising from the vibronic progression and from the LAM potentials can be achieved by employing the high-resolution results for the Franck−Condon (FC) active vibrations as available from the molecular beam experiments. The distribution along the LAM coordinate often expresses itself in characteristic features of the band shape, which describes the broadening of the individual vibronic transitions. By means of a simultaneous FC and band shape analysis of the temperature dependent steady-state fluorescence spectra, the effective S_1 torsional potential (see Figure 1) could be determined for 9,9′-bianthryl (BA)[20] and some derivatives[21] in the nonpolar solvent 2-methylbutane.

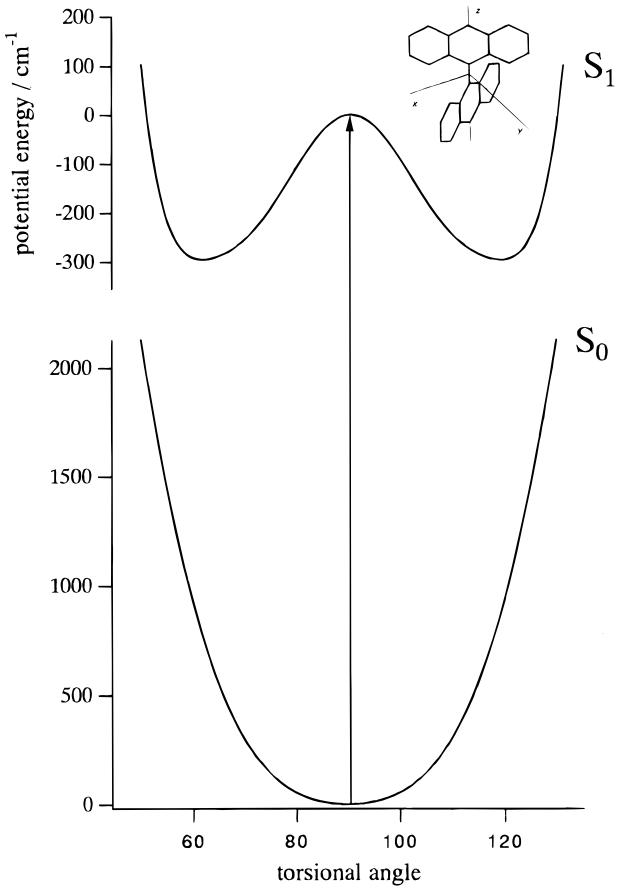

Figure 1. S_0 and S_1 torsional potentials of BA in methylcyclohexane calculated with the potential parameters listed in Table 1. The arrow represents transitions corresponding to excitation at the maximum of the first vibronic band of the absorption spectrum.

The photophysical properties of BA have been frequently studied since its dual fluorescence was discovered by Schneider and Lippert.[22] The strong red shift and broadening of the fluorescence spectrum observed in polar solvents are believed to be caused by the superposition of emission from a nonpolar excitonic and a polar charge transfer (CT) state. Though BA is a D_2 symmetric molecule with a vanishing dipole in the

[⊗] Abstract published in *Advance ACS Abstracts,* February 15, 1997.

S1089-5639(96)03910-2 CCC: $14.00

electronic ground state, it was proposed that the charge separation occurs because of spontaneous polarization of the solvent, which leads to a stabilization of the CT state by the reaction field.[23,24]

High-resolution studies on BA in a molecular beam[16−18] showed no evidence for a CT state. But they enabled a precise characterization of the S_0 and the S_1 torsional potential resulting in a double minimum potential for the nonpolar S_1 state. In molecular beam experiments on BA-solvent cluster[25,26] two different types of fluorescence were observed. The dispersed fluorescence spectrum of clusters with nonpolar molecules exhibits sharp bands and short fluorescence lifetimes similar to the isolated molecule. On the other hand, clusters with polar molecules show red-shifted, strongly broadened bands and elongated lifetimes that were interpreted to be due to the formation of the CT state. In the case of clusters with symmetric ketones both types of fluorescence were found, indicating the presence of two kinds of clusters with different arrangement of the solvent molecule.

Several time-resolved spectroscopic experiments on BA in different solvents have been performed to examine the effect of the solvent on the electronic structure and the dynamics of BA in the S_1 state.[27−34] The kinetics observed in polar solvents often matched those measured in experiments on solvation dynamics, suggesting that the formation of the CT state is controlled by the solvent relaxation, though, in some cases, a more complicated behavior was reported.[31] Only few facts are known on a possible interplay between the CT process and the torsional relaxation that is suggested by theoretical considerations.[24] In most of the previous studies the time-resolved fluorescence was analyzed at either a single or a few emission wavelengths. However, to get a more in-depth insight about the multiple processes involved in the excited state dynamics of BA, a quantitative analysis of the entire spectrum seems to be required that is based on an adequate model describing the effects of solvent and torsional dynamics as well as the vibronic progression. An approach partly accomplishing these conditions was proposed by Kang et al.[34] Though their model does not take explicitly account of the torsional relaxation.

Recently, we presented a quantitative interpretation of the marked excitation wavelength dependence of the steady-state fluorescence spectra of BA in a highly viscous nonpolar polymer.[35] Irradiation at the red edge of the absorption spectra results in a selective excitation of distinct conformers (i.e., subclass of molecules belonging to a narrow torsional distribution), which may be exploited to probe torsional relaxation. In this work, we subject the time-resolved fluorescence spectra of BA in nonpolar solvents to a band shape analysis. Since intermolecular interactions are of minor significance in these solvents, torsional relaxation is expected to predominantly cause the variation of the fluorescence spectra. This analysis provides a quantitative description of the effect of torsional relaxation on the fluorescence dynamics, which serves as a basis for a further-going study on the time-resolved fluorescence of BA in *n*-alcohols.[36]

Experimental Section

The preparation of 9,9′-bianthryl (BA) has already been described in ref 20. Spectrograde methylcyclohexane (MCH), Decalin (*cis*−*trans* mixture) (D), and isooctane (ISOO) were used without further purification. The samples were deoxygenated by N_2 bubbling and sealed afterward. The concentration of BA was about 8×10^{-3} mol m^{-3}.

The time-resolved spectra were measured by using a femtosecond Ti/Al_2O_3 laser (Spectra Physics, pulse autocorrelation fwhm of ∼100 fs, repetition rate of 82 MHz) that is tuneable between 740 and 810 nm. The samples were excited by the second harmonic generated with a BBO crystal at 388 nm (MCH) and 389 nm (D−ISOO mixture, 1:1). The fluorescence was detected by a two-dimensional syncroscan streak camera (Hamamatsu, C2909) operated at 82 MHz in conjunction with an imaging spectrograph (Chromex, 250IS). The time resolution of the experimental setup was about 15 ps and the spectral resolution about 1.6 nm. The fluorescence was observed under "magic angle" conditions. To minimize distraction from scattering light, a 390 nm cutoff filter was used.

The fluorescence spectra were corrected by calibrating the time-resolved spectra obtained at room temperature to the (corrected) steady-state fluorescence spectra of the same sample recorded on a Hitachi 850E fluorescence spectrophotometer. At room temperature no time dependent spectral change could be observed, indicating that the fluorescence measured under these conditions occurs from a steady state. Furthermore, the remaining fluorescence originating from the preceding detection cycle due to the long lifetime of BA (∼6 ns) was subtracted from the spectra.

Theory

In a preceding article[35] a semiclassical model was presented that provides a description of the time-resolved fluorescence of flexible molecules in liquid solution. This model applies to cases where the time dependent spectral change prevailingly arises from the motion along a single large amplitude motion (LAM) coordinate. Provided that the Born−Oppenheimer and the Condon approximation are appropriate, the time-resolved fluorescence spectrum can be represented by[20,35]

$$\Phi_{\tilde{\nu}}(\tilde{\nu}, t)/\tilde{\nu}^3 = {}^1/_3 C^{\mathrm{fl}} N_{\mathrm{E}}(t) |\mu^0_{\mathrm{EG}}|^2 \sum_{\mathrm{e}} \sum_{\mathrm{g}} W_{\mathrm{Ee}} (\mathrm{e}|\mathrm{g})^2 S^{\mathrm{fl}}_{\mathrm{EG}}(\tilde{\nu} - \tilde{\nu}^{0,\mathrm{fl}}_{\mathrm{eg}}, t) \quad (1)$$

$\Phi_{\tilde{\nu}}$ is the emitted spectral photon current density related to the wavenumber $\tilde{\nu}$, C^{fl} a constant, and N_{E} the total number of molecules in any excited vibronic state related to the probe volume. μ^0_{EG} is the electronic transition dipole at reference configuration between the electronic ground and the lowest excited state $|\mathrm{G}\rangle$ and $|\mathrm{E}\rangle$, respectively, and W_{Ee} is the Boltzmann factor describing the population of the excited vibronic states. $(\mathrm{e}|\mathrm{g})$ is the Franck−Condon overlap integral between the vibrational states $|\mathrm{g}\rangle$ and $|\mathrm{e}\rangle$ belonging to the ground and the excited electronic state, respectively. The semiclassical band shape $S^{\mathrm{fl}}_{\mathrm{EG}}$ describes the spectral broadening of each vibronic transition $|\mathrm{G}\rangle|\mathrm{g}\rangle \leftarrow |\mathrm{E}\rangle|\mathrm{e}\rangle$ caused by intramolecular as well as intermolecular effects and is given by[20]

$$S^{\mathrm{fl}}_{\mathrm{EG}}(\tilde{\nu} - \tilde{\nu}^{0,\mathrm{fl}}_{\mathrm{eg}}, t) = \int_0^{\pi} \mathrm{d}\varphi \; w^{\mathrm{L}}_{\mathrm{E}}(\varphi, t) p^{\mathrm{fl}}_{\mathrm{EG}}(\tilde{\nu} - \tilde{\nu}^{\mathrm{fl}}_{\mathrm{eg}}(\varphi, t), t) \quad (2)$$

$$\tilde{\nu}^{\mathrm{fl}}_{\mathrm{eg}}(\varphi, t) = \tilde{\nu}^0_{\mathrm{eg}} + \Delta\tilde{\nu}^{0,\mathrm{fl}}_{\mathrm{eg}}(t) + V^{\mathrm{L}}_{\mathrm{E}}(\varphi) - V^{\mathrm{L}}_{\mathrm{G}}(\varphi)$$

The superscript "L" typifies quantities depending on the torsional (LAM) degree of freedom. $w^{\mathrm{L}}_{\mathrm{E}}$ is the normalized probability distribution function with respect to the torsional angle φ (torsional distribution) in the excited electronic state. $p^{\mathrm{fl}}_{\mathrm{EG}}$ summarizes spectral shift and broadening effects caused by librations and intermolecular interaction. It may be empirically described by a Gaussian with the width σ^{fl}. $\tilde{\nu}^0_{\mathrm{eg}}$ is the transition frequency at reference configuration with respect to the torsional angle (reference conformation) immediately after excitation. $\Delta\tilde{\nu}^{0,\mathrm{fl}}_{\mathrm{eg}}$ accounts for a solvent-induced shift of $\tilde{\nu}^0_{\mathrm{eg}}$. $V^{\mathrm{L}}_{\mathrm{G}}$ and $V^{\mathrm{L}}_{\mathrm{E}}$ are the torsional potentials in the electronic states $|\mathrm{G}\rangle$ and $|\mathrm{E}\rangle$, respectively, which may be represented by a Fourier

series of the form [21,37]

$$V_I^{\mathrm{L}}(\varphi) = \sum_n V_{2nI}((-1)^n - \cos 2n\varphi) \quad I = \mathrm{G, E} \qquad (4)$$

where V_{2nI} are expansion coefficients.

On condition that the torsional motion may be treated as an overdamped motion (high-friction regime), the time evolution of the torsional distribution can be described by a Smoluchowski type equation. Assuming the decay rate to be independent of the torsional angle and by neglect of any coupling between the torsional and the overall rotational motion, the following equation holds for the excited-state torsional distribution of a solute molecule consisting of two equal parts.[35]

$$\frac{\partial w_{\mathrm{E}}^{\mathrm{L}}(\varphi, t)}{\partial t} = \frac{2k_{\mathrm{B}}T}{\zeta}\frac{\partial^2 w_{\mathrm{E}}^{\mathrm{L}}(\varphi, t)}{\partial \varphi^2} + \frac{2}{\zeta}\frac{\partial}{\partial \varphi}\left(\frac{\partial V_{\mathrm{E}}^{\mathrm{L}}(\varphi)}{\partial \varphi} w_{\mathrm{E}}^{\mathrm{L}}(\varphi, t)\right) + k_{\mathrm{abs}}(t)(w_{\mathrm{E}}^{\mathrm{L,FC}}(\varphi, \tilde{\nu}_{\mathrm{ex}}) - w_{\mathrm{E}}^{\mathrm{L}}(\varphi, t)) \qquad (5)$$

ζ is the friction coefficient of one anthracene moiety, k_{B} the Boltzmann constant, and T the temperature. The quantity k_{abs} is related to the time profile of the exciting laser pulse and is given explicitly in ref 35. $w_{\mathrm{E}}^{\mathrm{L,FC}}$ is the Franck−Condon excited-state torsional distribution created by the excitation process that depends mainly on the excitation wavenumber $\tilde{\nu}_{\mathrm{ex}}$ and the equilibrium torsional distribution in the electronic ground-state $w_{\mathrm{G}}^{\mathrm{L,eq}}$. In the case of excitation near the 0_0^0 transition $w_{\mathrm{E}}^{\mathrm{L,FC}}$ can be approximated by the following equation provided that the 0_0^0 transition is sufficiently separated from other vibronic transitions:[35]

$$w_{\mathrm{E}}^{\mathrm{L,FC}}(\varphi, \tilde{\nu}_{\mathrm{ex}}) = K(\tilde{\nu}_{\mathrm{ex}}) w_{\mathrm{G}}^{\mathrm{L,eq}}(\varphi) \int \mathrm{d}\tilde{\nu}\, A(\tilde{\nu} - \tilde{\nu}_{\mathrm{ex}}) p_{\mathrm{EG}}^{\mathrm{abs}}(\tilde{\nu} - \tilde{\nu}_{00}^{\mathrm{abs}}(\varphi)) \qquad (6)$$

K is a normalization constant, A is the spectral band shape of the exciting light, and $p_{\mathrm{EG}}^{\mathrm{abs}}$ accounts for intermolecular broadening related to the absorption process. As in the case of emission, it may be represented by a Gaussian with the width σ_{abs}. On condition that the duration of the exciting light pulse is short compared with the time scale characterizing the torsional relaxation, k_{abs} can be approximated by the Dirac delta function. Equation 5 reduces then to an initial value problem including the first two terms with the initial distribution $w_{\mathrm{E}}^{\mathrm{L,FC}}$.

Results and Discussion

We have studied the time-resolved fluorescence spectra of 9,9′-bianthryl (BA) in methylcyclohexane (MCH) at several temperatures in the range 127−200 K. To increase the accessible viscosity range, the time-resolved fluorescence was also investigated in a Decalin−isooctane (1:1) mixture (D−ISOO) between 150 and 170 K. Thus, the total viscosity covered by these combinations reaches from ∼6 mPa s to ∼3500 mPa s.[38,39] As mentioned in the Introduction, the variation of the excitation wavenumber within the red edge of the first vibronic band of the absorption spectra enables the selective excitation of distinct conformers. Irradiation at the maximum of the first vibronic band gives rise to a narrow initial torsional distribution centered around $\varphi = 90°$.[35] Proceeding in this manner, the effect of torsional relaxation should manifest itself most distinctly in the fluorescence spectra.

The fluorescence spectra of BA in MCH at 127, 143, and 160 K are displayed in the Figures 2−4. As a common feature of all spectra, a continuous loss of structure and a red shift of the band centers can be observed with increasing time. The spectral changes appear most clearly within the range of the first vibronic band. This is due to the fact that the 0_0^0 transition, which contributes predominantly to this band, is well separated from other vibronic transitions, and therefore, the alteration of the band shape is most pronounced. As it is evident from the pictures, an increase of the viscosity entails a slowing down of the observed spectral changes. So, for example, comparing the spectra of BA in MCH at 143 and 127 K shows the similarity between the spectral features during the first 75 ps at the former temperature and those measured between 200 and 400 ps at the latter temperature. In the regime of lower viscosity (MCH, >170 K) the temporal evolvement of the spectra stagnates at advanced time, indicating that the solute molecules undergoing torsional relaxation reached the thermal equilibrium state within the period of observation.

To obtain more quantitative information on the underlying torsional dynamics, the spectra were subjected to a band shape analysis based on the semiclassical model presented in the previous chapter. However, a satisfactory reproduction of the experimental spectra could be achieved only when further assumptions specified below were taken into consideration. So the spectra measured at high viscosity (e.g., MCH, 127 K) already show a rather large broadening at the earliest time (15 ps), suggesting that the torsional relaxation occurs to a considerable extent during the first few picoseconds. On the other hand, the small temporal variation of the spectra during the period of observation reveals a comparatively slow progress of the subsequent torsional relaxation. These findings can be interpreted by assuming a solvent "cage" structure, which allows for an initial almost unhindered torsional motion. In the sequel the increasing interaction with the solvent molecules retards the torsional relaxation until the solute molecules experience the full hydrodynamic drag of the solvent. The time scale of the initial inertial motion may be estimated by using the streaming frequency[40] $\omega_{\mathrm{s}} = (k_{\mathrm{B}}T/I_{\mathrm{rel}})^{1/2}$. Employing a value of 9×10^{-45} J s^2 for the reduced moment of inertia[35] and $T = 150$ K results in $\omega_{\mathrm{s}} \approx 5 \times 10^{11}$ s^{-1}.

To adapt the model to this observed behavior, it was modified in an empirical manner by subdividing the relaxation process into two steps. The fast initial relaxation was treated according to eq 5 by introducing an effective friction coefficient ζ_{initial}, which is much smaller than the friction coefficient for longer times. The time evolution of the torsional distribution was calculated for a (reduced) time period $\delta = t/\zeta_{\mathrm{initial}}$. From the time resolution of the experiment ($t \approx 20$ ps) one can estimate the upper limit $\zeta_{\mathrm{initial}} < 100$ cm^{-1} ns. The torsional motion during the observation period at times $t > 20$ ps was assumed to experience the full hydrodynamic drag. The friction coefficient governing this second part of the torsional relaxation should therefore depend strongly on the viscosity.

The results of the band shape analysis are shown in the Figures 2−4. Deviating from the practice in previous studies,[20,21] we chose a representation of the spectra employing Φ_λ (emitted spectral photon current density related to the wavelength), which is linked to $\Phi_{\tilde{\nu}}$ by $\Phi_\lambda = \Phi_{\tilde{\nu}}\tilde{\nu}^2$. A good correspondence of the experimental and the simulated fluorescence spectra could be achieved for all temperatures in both solvents. Especially, the features of the first vibronic band are well reproduced by the simulated spectra. So, for example, all spectra exhibit a shoulder at the blue edge, which arises from transitions of solute molecules with perpendicular conformation. The decrease of this shoulder, which represents a characteristic attribute of the time dependent band shape (see Figure 5), reflects the diminution of the S_1 torsional distribution within the range of the potential barrier at $\varphi = 90°$.

The simulation of the spectra were performed according to eqs 1 and 2 (for details see ref 20). The initial torsional

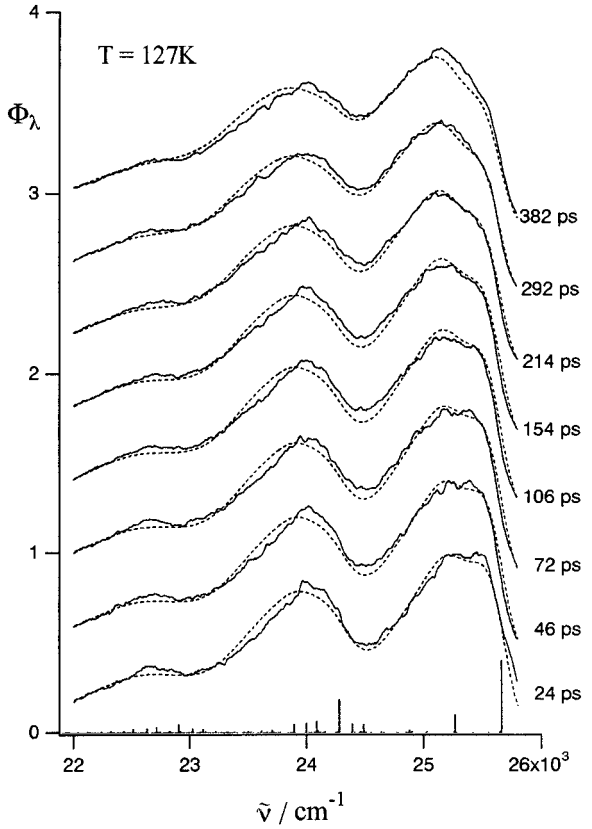

Figure 2. Experimental (−) and simulated (- - -) fluorescence spectra of BA in methylcyclohexane at $T = 127$ K. The vibronic structure is indicated by a line spectrum. Spectra at consecutive times are displayed with an ordinate shift of 0.4.

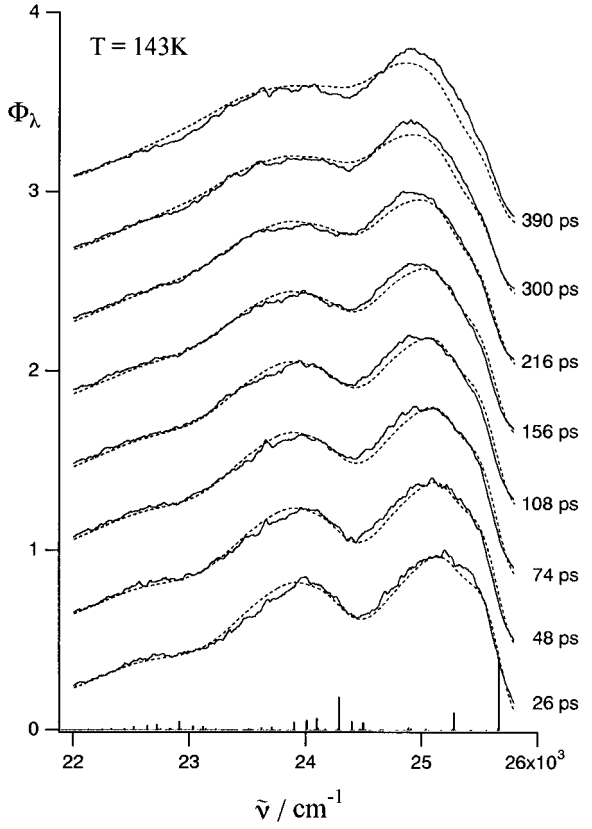

Figure 3. Experimental (−) and simulated (- - -) fluorescence spectra of BA in methylcyclohexane at $T = 143$ K. Legend is as in Figure 2.

distribution was calculated according to eq 6 assuming a Gaussian profile for the exciting light pulse with a width $\sigma_{ex} = 50$ cm^{-1}. The whole procedure requires the specification of several model parameters listed in the following. The parameters determining the Franck−Condon (FC) progression (cf. line spectra in Figures 2−4), i.e., the vibrational frequencies and the displacement parameters of five degenerate normal modes, were taken unaltered from ref 20. The time dependent band shape itself is characterized by the parameters specifying the S_0 and the S_1 torsional potential V_{2nG} and V_{2nE} (cf. eq 4), respectively, the friction coefficient ζ, and the parameter δ specifying the extent of the initial fast torsional relaxation. In accordance with previous studies the potential parameters V_{2G} and V_{4G}, as obtained from the analysis of the free jet spectra (cf. refs 18 and 20), were used assuming the S_0 potential to be unaffected by solvent interaction. Apart from the temporal spectral change due to the torsional relaxation a small solvent-induced shift (Stokes shift) $\Delta\tilde{\nu}_{00}^{0,fl}$ (cf. eq 3) has to be taken into account whose time dependence was approximated by a single exponential with time constant τ_s and amplitude Δ_s (see legend of Table 1). The 0_0^0 transition wavenumbers $\tilde{\nu}_{00}^0$ were estimated from the absorption spectra.

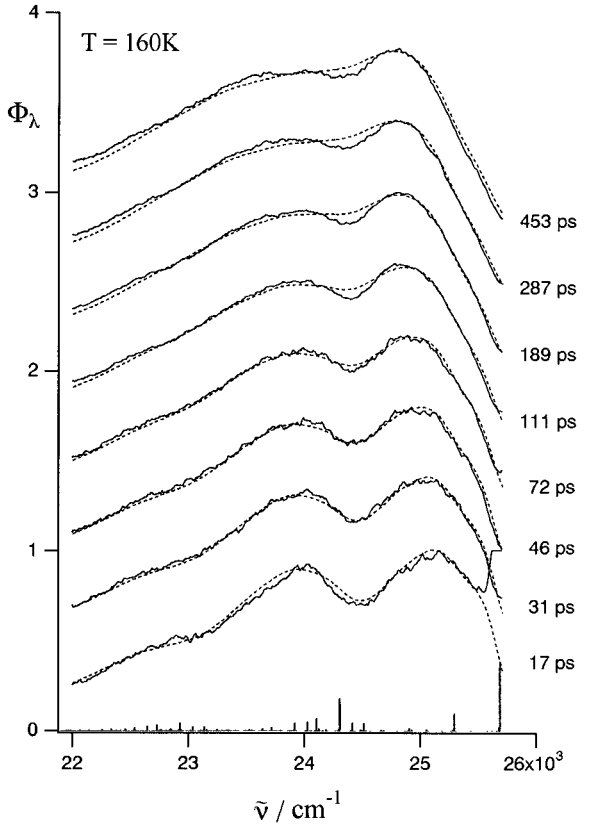

Figure 4. Experimental (−) and simulated (- - -) fluorescence spectra of BA in methylcyclohexane at $T = 160$ K. Legend is as in Figure 2.

The S_1 potential parameters V_{2nE} and the parameter ζ and δ were optimized by using the Levenberg−Marquardt algorithm[41] and are listed in Table 1. Separate optimization of the potential parameter for each temperature did not show any significant dependence of the S_1 torsional potential on the temperature. Therefore, the band shape analysis was done with a common set of S_1 potential parameters for each solvent. As a result, almost identical S_1 torsional potentials were determined for BA in MCH and in D−ISOO. In both cases, the height of the local barrier at perpendicular conformation and the minimum angle were found to be $\Delta V \approx 300$ cm^{-1} and $\varphi_{min} \approx 62°$, respectively. These values are in good accordance with previous results for 2-methylbutane[42] ($\Delta V \approx 280$ cm^{-1}, $\phi_{min} \approx 62°$) and for polyisobutene[35] ($\Delta V \approx 325$ cm^{-1}, $\phi_{min} \approx 61°$). However, the shape of the potential barrier was found to be more narrow and peaked compared with previous results. This indicates the enhanced sensitivity of the analysis of time-resolved spectra with

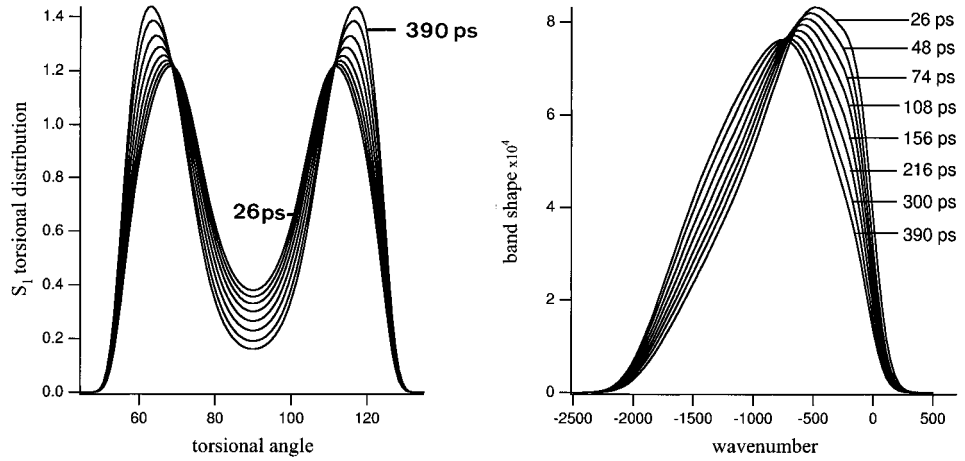

Figure 5. Calculated S_1 torsional distributions and fluorescence band shapes as a function of time for BA in methylcyclohexane at $T = 143$ K. With increasing time the torsional distributions evolves toward $\phi_{min} = 62°$ (118°).

TABLE 1: Model Parameters[a] Used in the Simulation of the Time-Resolved Fluorescence Spectra of 9,9′-Bianthryl (BA) in Methylcyclohexane (MCH) and in a Decalin−Isooctane (D−ISOO) Mixture[e]

	V_2 (cm^{-1})	V_4 (cm^{-1})	V_6 (cm^{-1})	V_8 (cm^{-1})	V_{10} (cm^{-1})	V_{12} (cm^{-1})	ΔV (cm^{-1})	ϕ_{min}
S_0[b]	−5160	−1100	0	0	0	0	90°	
S_1 MCH	−6075	−1517	1553	1599	700	108	299	62, 118°
S_1 D−ISOO	−5944	−1366	1608	1536	612	76	297	62, 118°

T (K)	η[c] (mPa s)	ζ (cm^{-1} ns)	δ (10^{-3} cm^{-1})	$\tilde{\nu}^0_{00}$ (cm^{-1})	σ^{fl} (cm^{-1})	τ_s[d] (ps)	Δ_s[d] (cm^{-1})
			MCH				
200	6.22	200	0.198	25 715	130	<15	80
190	9.43	310	0.194	25 708	130	<15	80
180	15.5	425	0.187	25 700	130	<15	100
170	28.7	580	0.185	25 692	125	16	100
160	61.3	785	0.167	25 684	125	22	100
150	158	1500	0.158	25 676	120	26	100
143	351	2900	0.154	25 670	120	27	80
132	−	6000	0.136	25 661	115	42	70
127	-	7250	0.116	25 655	115	37	50
			D−ISOO				
170	254	2300	0.152	25 656	125	23	100
160	750	6300	0.127	25 648	120	40	100
150	3500	15000	0.128	25 640	120	40	100

[a] FC parameters are the same as for BA in Table 1 of ref 20. [b] Taken from refs 18 and 20. [c] Taken from refs 38 and 39. [d] The parameters Δ_s and τ_s describe the solvent-induced shift by $\Delta\tilde{\nu}^{0,fl}_{eg}(t) = \Delta_s(1 - \exp(-t/\tau_s))$. [e] Experimental errors of the model parameters were estimated to be about 5%.

respect to details of the S_1 torsional potential. Consequently, a minimum of six parameters is required for a sufficient characterization of the S_1 torsional potential. The parameter δ was found to increase with the temperature, which seems to be reasonable. Though δ has no well-defined physical meaning, it may be related to the free volume attached to each solute molecule. The resulting values for the friction coefficient ζ are represented in Figure 6 as a function of the viscosity η. A good fit of the data could be achieved by the phenomenological power law of the form $\zeta = B\eta^a$. The fit yields an exponent $a = 0.62 \pm 0.05$ (0.70 ± 0.12) for BA in MCH (D−ISOO). Considering the large uncertainty in the latter case, there seems to be no significant dependence of a on the solvent. The joint fit of the data of both solvents gives a value $a = 0.67 \pm 0.04$, though the data suggest slightly higher ζ values for D−ISOO at equal viscosity. As mentioned above, a small spectral shift Δ_s due to interaction with the surrounding solvent molecules had to be taken into account. The time constant τ_s for this process is fast compared with the torsional relaxation time and could be identified in all spectra. A slight increase of τ_s with increasing viscosity was observed (cf. Table 1).

The analysis shows that the dynamics disclosed by the fluorescence spectra can be predominately ascribed to the torsional relaxation. In particular, the characteristic variation of the first vibronic band directly points out the temporal change

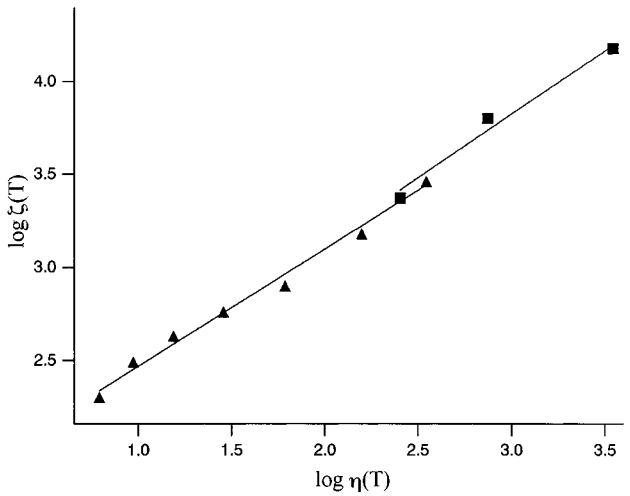

Figure 6. Representation of the friction coefficient ζ related to the torsional motion as obtained from the band shape analysis vs the solvent viscosity η for BA in MCH (△) and in D−ISOO (□).

of the band shape, which reflects the motion of the S_1 torsional distribution toward the potential minimum. The band shape itself shows a red shift and a broadening with increasing time because of the smaller transition wavenumber and the larger

slope of the S_0 torsional potential with increasing deviation from $\phi = 90°$. On the other hand, solvent relaxation, which contributes only to a minor extent, causes a shift of the whole spectrum without affecting its shape. The magnitude of the shift ($\sim$100 cm^{-1}) suggests that mainly dispersion interaction gives rise to the solvent dynamics, as expected for nonpolar solvents. Furthermore, the experimental results confirmed that the specific choice of the excitation wavenumber is of crucial importance in order to obtain maximum information about the underlying relaxation processes. So, for example, irradiation at the second vibronic band of the absorption spectrum results in much less pronounced spectral changes.

Another worth mentioning outcome of this study refers to the relation between the friction coefficient and the viscosity. In a wide range of isomerization studies[1] a weak dependence of the barrier-crossing rate coefficient k_{iso} on the viscosity according to the relation $k_{iso} \approx \eta^{-a}$ with $a < 1$ was observed. Three alternative approaches were frequently discussed in the literature to account for the deviation from linear dependency predicted by Kramers' model[43] in conjunction with the hydrodynamic approximation: (1) coupling between the reactive mode and other modes, which requires a multidimensional treatment,[44] (2) the presence of a frequency dependent friction,[13,45] and (3) the divergence between the microviscosity effecting the isomerization reaction and the medium viscosity (breakdown of the Stokes−Einstein hydrodynamic approximation). For BA, the one-dimensional treatment of the torsional motion seems to be appropriate. There is no indication for a coupling with other large amplitude motion (LAM) modes from the high-resolution spectra.[18] Frequency dependent friction has been suggested to be relevant to reactions distinguished by a high barrier with a strong curvature. Such effects should be of minor importance for BA, which shows a comparatively shallow potential barrier. On the other hand, the presence of an initial fast component points out that the hydrodynamic approximation provides an inadequate description for the torsional relaxation of BA. So small systematic deviations of the simulated spectra from the experimental ones could be due to a more continuous increase of the friction coefficient instead of the simple two-step behavior assumed in this simulation. The insufficiency of the hydrodynamic approximation was also suggested by studies on the isomerization of 1,1′-binaphthyl in alkanes.[7,46]

The results presented in this study may serve as a basis for the analysis of the time-resolved fluorescence of BA in *n*-alcohols, which was suggested to be predominantly determined by the formation of a charge transfer (CT) state.[29,31] Since the time scale of torsional relaxation is much smaller than those of solvent relaxation for these solvents, the effect of the torsional distribution on the CT state formation may be examined. The complicated relaxation behavior of these systems observed by Anthon and Clark[31] might be partly attributed to the involvement of torsional relaxation. The time-resolved fluorescence spectra of BA in *n*-hexanol at 273 K published by these authors suggest that the relaxation process takes place in two steps. On a time scale of about 10−100 ps the spectral change occurs almost without any decrease of the integral emission intensity, while at longer times a strong decrease can be observed. The time constant of the fast process ($\tau_3 = 62$ ps) corresponds roughly to the time scale of the torsional relaxation obtained for BA in MCH at 200 K ($\sim$50 ps), whereas the viscosity is almost equal for both systems. The strong decrease of the integral emission intensity ($\tau_2 = 519$ ps) may be attributed to the supposed formation of the CT state, though the reported spectra are too coarse-grained for additional conclusions. An in-depth investigation of this topic is in progress.[36]

Acknowledgment. K.E. thanks the Japan Society for the Promotion of Science (JSPS) for support through a postdoctoral fellowship. This work was partly supported by a Grant-in-Aid for New Program (06NP0301) to T.O. from the Ministry of Education, Science and Culture of Japan.

References and Notes

(1) Fleming, G. R. *Chemical Applications of Ultrafast Spectroscopy*; Oxford University Press: New York, 1986; p 179.
(2) Ito, M. *J. Phys. Chem.* **1987**, *91*, 517.
(3) Grabowski, Z. R.; Rotkiewicz, K.; Siemiarczuk, A.; Cowley, D. J.; Baumann, W. *Nouv. J. Chim.* **1979**, *3*, 443.
(4) Barbara, P. F.; Brus, L. E.; Rentzepis, P. M. *J. Am. Chem. Soc.* **1980**, *102*, 5631.
(5) Suzuki, T.; Mikami, N.; Ito, M. *J. Phys. Chem.* **1986**, *90*, 6431.
(6) Sundström, V.; Gillbro, T. *J. Chem. Phys.* **1984**, *81*, 3463.
(7) Bowman, R. M.; Eisenthal, K. B.; Millar, D. P. *J. Chem. Phys.* **1988**, *89*, 762.
(8) Rothenberger, G.; Negus, D. K.; Hochstrasser, R. M. *J. Chem. Phys.* **1983**, *79*, 5360.
(9) Courtney, S. H.; Fleming, G. R. *J. Chem. Phys.* **1985**, *83*, 215.
(10) Park, N. S.; Waldeck, D. H. *J. Chem. Phys.* **1989**, *91*, 943.
(11) Sun, Y.-P.; Saltiel, J.; Park, N. S.; Hoburg, A. E.; Waldeck, D. H. *J. Phys. Chem.* **1991**, *95*, 10336.
(12) Mohrschladt, R.; Schroeder, J.; Schwarzer, D.; Troe, J.; Vöhringer, P. *J. Chem. Phys.* **1994**, *101*, 7566.
(13) Grote, F.; Hynes, J. T. *J. Chem. Phys.* **1980**, *73*, 2715.
(14) Im, H.-S.; Bernstein, E. R. *J. Chem. Phys.* **1988**, *88*, 7337.
(15) Jonkman, H. T.; Wiersma, D. A. *J. Chem. Phys.* **1984**, *81*, 1573.
(16) Yamasaki, K.; Arita, K.; Kajimoto, O. *Chem. Phys. Lett.* **1986**, *123*, 1302.
(17) Khundkar, L. R.; Zewail, A. H. *J. Chem. Phys.* **1986**, *84*, 1302.
(18) Subaric-Leitis, A.; Monte, C.; Roggan, A.; Rettig, W.; Zimmermann, P.; Heinze, J. *J. Chem. Phys.* **1990**, *93*, 4543.
(19) Monte, C.; Roggan, A.; Subaric-Leitis, A.; Rettig, W.; Zimmermann, P.; *J. Chem. Phys.* **1993**, *98*, 2580.
(20) Wortmann, R.; Elich, K.; Lebus, S.; Liptay, W. *J. Chem. Phys.* **1991**, *95*, 6371.
(21) Elich, K.; Lebus, S.; Wortmann, R.; Petzke, F.; Detzer, N.; Liptay, W. *J. Phys. Chem.* **1993**, *97*, 9947.
(22) Schneider, F.; Lippert, E. *Ber. Bunsen-Ges. Phys. Chem.* **1968**, *72*, 1155.
(23) Beens, H.; Weller, A. *Chem. Phys. Lett.* **1969**, *3*, 666.
(24) Lippert, E.; Rettig, W.; Bonacic-Koutecky, V.; Heisel, F.; Miehe, J. A. *Adv. Chem. Phys.* **1987**, *68*, 1.
(25) Honma, K.; Arita, K.; Yamasaki, K.; Kajimoto, O. *J. Chem. Phys.* **1991**, *94*, 496.
(26) Honma, K.; Kajimoto, O. *J. Chem. Phys.* **1994**, *101*, 1752.
(27) Nakashima, N.; Murakawa, M.; Mataga, N. *Bull. Chem. Soc. Jpn.* **1976**, *49*, 854.
(28) Migita, M.; Okada, T.; Mataga, N.; Sakata, Y.; Misumi, S.; Nakashima, N.; Yoshihara, K. *Bull. Chem. Soc. Jpn.* **1981**, *54*, 3304.
(29) Mataga, N.; Yao, H.; Okada, T.; Rettig, W. *J. Phys. Chem.* **1989**, *93*, 3383.
(30) Okada, T.; Nishikawa, S.; Kanaji, K.; Mataga, N. In *Ultrafast Phenomena VII*; Harris, C. B., Ippen, E. P., Mourou, G. A., Zewail. A. H., Eds.; Springer-Verlag: Berlin, 1990; p 397.
(31) Anthon, D. W.; Clark, J. H. *J. Phys. Chem.* **1987**, *91*, 3530.
(32) Kang, T. J.; Kahlow, M. A.; Giser, D.; Swallen, S.; Nagarajan, V.; Jarzeba, W.; Barbara, P. F. *J. Phys. Chem.* **1988**, *92*, 6800.
(33) Barbara, P. F. In *Ultrafast Phenomena VII*; Harris, C. B., Ippen, E. P., Mourou, G. A., Zewail. A. H., Eds.; Springer-Verlag: Berlin, 1990; p 393.
(34) Kang, T. J.; Jarzeba, W.; Barbara, P. F.; Fonseca, T. *Chem. Phys.* **1990**, *194*, 81.
(35) Elich, K.; Wortmann, R.; Petzke, F.; Liptay, W. *Ber. Bunsen-Ges. Phys. Chem.* **1994**, *98*, 1263.
(36) Elich, K.; Okada, T. Manuscript in preparation.
(37) Lewis, J. D.; Malloy, T. B.; Chao, T. H.; Laane, J. *J. Mol. Struct.* **1972**, *12*, 427.
(38) Ruth, A. A.; Nickel, B.; Lesche, H. *Z. Phys. Chem.* **1992**, *175*, 91.
(39) von Salis, G. A.; Labhart, H. *J. Phys. Chem.* **1968**, *72*, 752.
(40) Nordio, P. L.; Polimeno, A. *Chem. Phys.* **1994**, *180*, 109.
(41) Press, W. H.; Flannery, B. P.; Teukolsky, S. A.; Vetterling, W. T. *Numerical Recipes in C*; Cambridge University Press: Cambridge, 1992; p 683.
(42) Wortmann, R.; Lebus, S.; Elich, K.; Assar, S.; Detzer, N.; Liptay, W. *Chem. Phys. Lett.* **1992**, *198*, 220.
(43) Kramers, H. A. *Physica* **1940**, *7*, 284.
(44) Agmon, N.; Kosloff, R. *J. Phys. Chem.* **1987**, *91*, 1988.
(45) Velsko, S. P.; Waldeck, D. H.; Fleming, G. R. *J. Chem. Phys.* **1983**, *78*, 249.
(46) Canonica, S.; Wild, U. P. *J. Phys. Chem.* **1991**, *95*, 6535.